AIAA JOURNAL
Vol. 32, No. 1, January 1994

Pressure Measurements on a Pitching Airfoil in a Water Channel

Rand N. Conger*
John Graham Associates, Seattle, Washington 98101
and
B. R. Ramaprian†
Washington State University, Pullman, Washington 99164

Measurements of unsteady pressures over a symmetric NACA 0015 airfoil performing pitching maneuvers are reported. The tests were performed in an open-surface water channel specially constructed for this purpose. The design of the apparatus allowed the pressure measurements to be made to a very high degree of spatial and temporal resolution. Reynolds numbers in the range of 5.2×10^4 to 2.2×10^5 were studied. Although the results qualitatively agreed with earlier studies performed at similar Reynolds numbers, the magnitudes of pressure and aerodynamic forces measured were observed to be much larger than those measured in earlier pitchup studies. They were found, in fact, to be closer to those obtained in some recent high-Reynolds-number experiments. This interesting behavior, which was suspected to be caused by the relatively high freestream turbulence level in the water channel, was explored in some detail. In addition, several issues like the quasisteady and dynamic effects of the pitching process are discussed. The experimental data are all archived and are available for use as a database.

Nomenclature

C_l = coefficient of lift, $l/(\rho U_\infty^2/2)c$
C_p = coefficient of pressure, $(P - P_\infty)/(\rho U_\infty^2/2)$
c = airfoil chord
l = lift force per unit span
P = instantaneous pressure at a point on the model surface
P_∞ = freestream static pressure
Re = Reynolds number, $U_\infty c/\nu$
t = time
U_∞ = freestream velocity
x = chordwise location along the airfoil, $x = 0$ at nose
α = angle of incidence
α_i = initial angle of incidence
α^+ = nondimensional pitch rate, $\omega c/U_\infty$
ν = kinematic viscosity
ρ = density
ω = angular velocity of pitching

Introduction

Background

THE two-dimensional unsteady flowfield around an airfoil undergoing a pitchup motion at constant angular velocity in a steady stream exhibits several features that are of interest in the study of supermaneuverability of fighter aircraft. Several studies reported to date[1-12] have shown that much higher lift is generated by a pitching airfoil compared with a stationary airfoil and that stall is delayed until angles of attack much higher than in steady state. These effects have been observed to occur in conjunction with the formation of large-scale vortical structures on the suction side of the airfoil.

Experiments on pitching airfoils have so far generally involved (with the exception of Ref. 6) the measurement of pressure distribution over the airfoil surface. In general, these experiments have been performed in wind tunnels, with the exception of the towing-tank studies of Graham and Yeow[11] and Strickland and Graham.[12] Those studies have been conducted at low Reynolds numbers, $0.2\text{–}2.5 \times 10^5$ on NACA 0012 or NACA 0015 airfoil sections. The only high-Reynolds-number studies reported on constant-velocity pitching are those of Lorber and Carta[5] on a Sikorsky SSC-A09 airfoil at Reynolds numbers on the order of $2\text{–}4 \times 10^6$, but at relatively low pitch rates.

The aforementioned studies have generally led to a fairly consistent qualitative picture of the evolution of the surface pressure distribution and the aerodynamic forces and moments. They have shown that the dynamics are strongly influenced by the nondimensional pitch rate α^+. However, there is a lack of quantitative consistency among the different experiments in several respects. The magnitudes of the pressures measured in the low-Reynolds-number studies were significantly lower than those measured in the experiments of Lorber and Carta[5] at high Reynolds numbers and much lower pitch rates. In fact, there is considerable discrepancy between even the steady-state lift slopes reported in some low-Reynolds-number pitchup studies and those reported for high-Reynolds-number flows, both in the classical literature (i.e., Abbot and Von Doenhoff[13]) and in more recent studies (e.g., Piziali[14] and McAlister and Takahashi[15]). Francis and Keesee[3] and Jumper et al.[4] observed steady-state lift slopes of much smaller magnitude than those found for the respective airfoils at high Reynolds numbers. Walker et al.[9] observed *unsteady* lift slopes at low pitch rates of significantly lower magnitude than the classical *steady* lift slopes. In fact, a survey of the literature shows that there are some discrepancies in the magnitudes of surface pressures and aerodynamic forces reported in different studies on the same airfoil section (NACA 0015). It is not clear whether the aforementioned apparent quantitative discrepancies are due to the poor spatial resolution of the pressure data, inadequate dynamic response of the pressure measurement instrumentation, or some more fundamental reason that is not well understood at this time.

Motivation and Scope of the Present Work

The present study is a part of a larger project aimed at addressing the issues just outlined. The work presented in this

Received June 1, 1992; presented as Paper 93-0814 at the AIAA 31st Aerospace Sciences Meeting, Reno, NV, Jan. 11-14, 1993; revision received June 15, 1993; accepted for publication June 21, 1993.

*Engineer.
†Professor, Department of Mechanical and Materials Engineering.

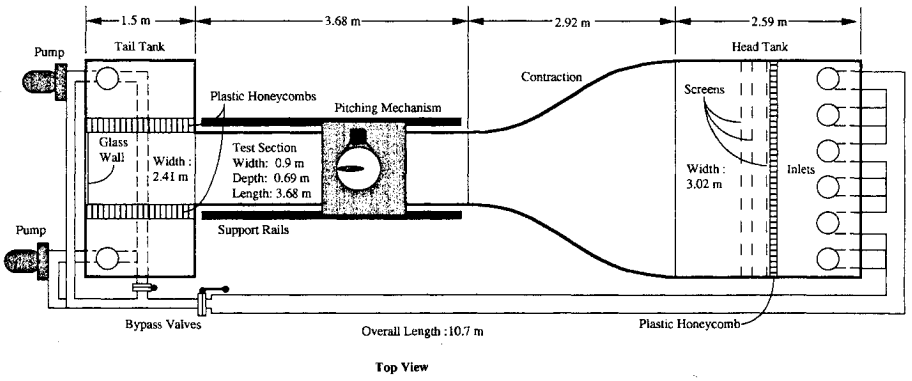

Fig. 1 Experimental facility.

paper involved the measurements of the surface pressure measurements on the pitching airfoil. The main focus of the study is on angles of incidence up to and slightly beyond the initiation of the dynamic stall process, although, in some cases, data have been obtained well into the postdynamic stall region. The experiments were performed using a relatively large NACA 0015 airfoil in a water channel. Surface pressures have been obtained at a fine spatial resolution over the airfoil. The use of a water channel permits Reynolds numbers on the order of 10^5 to be attained at very low freestream velocities (on the order of 30 cm/s). The low freestream velocities increase the time scales involved in the pitching process and make it possible to obtain measurements with a fine temporal resolution. Also, the use of the water channel allows one to use particle image velocimetry (PIV) for measuring the instantaneous velocities in the flow around the airfoil. These measurements, however, have been reported separately.[16]

This paper should be of interest to the researchers in this area for two reasons: 1) pressure data have been obtained on a pitching airfoil to a degree of spatial and temporal resolution better than has hitherto been possible, by using a facility, instrumentation, and experimental procedure different from those used in earlier studies; and 2) the present experimental conditions seem to simulate (as will be seen later) wind-tunnel tests at much higher Reynolds numbers. This latter point is interesting from an academic as well as a practical viewpoint.

Experimental Particulars

Experimental Setup

The experiments were performed in a recirculating open-surface water channel with a cross-sectional area of 0.9×0.7 m, specially designed for this study. Figure 1 shows a schematic of the facility. The entire facility is constructed of nonferrous materials to prevent rust formation. The water quality is carefully controlled through the use of a water softener, a micron-sized filter, periodic chlorination, and pH management. The bottom and sides of the test section are constructed of glass to provide a full view of the phenomena under study. The flow in the test section can be varied from approximately 3 to 50 cm/s. The freestream turbulence in the channel at a velocity of 30 cm/s was measured to be 0.8%. A detailed description of the water channel is provided in Conger and Ramaprian.[17] The test model is a NACA 0015 airfoil with a 36-cm chord and 60-cm span mounted vertically in the channel. The airfoil is nearly hollow and is constructed of a single piece of extruded aluminum with a 64-cm diameter Plexiglas end plate on its upper edge. The airfoil is positioned with its quarter-chord point and pitch axis aligned with the center of the plate. A 1.9-cm gap separates the lower edge of the airfoil from the floor of the channel. Figure 2 shows a schematic of the test setup. The transparent end plate, which dips slightly into the water, not only serves to eliminate three-dimensional effects due to the presence of a free surface but also makes it possible to obtain photographs of the flowfield

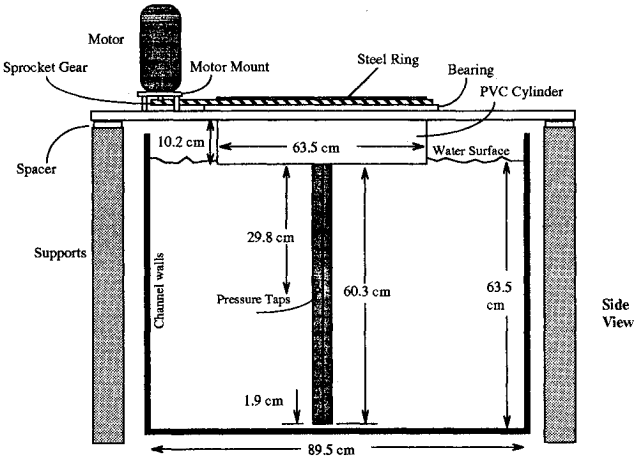

Fig. 2 Airfoil pitching mechanism.

without any optical distortions caused by the free surface. Pitching motions are imparted to the airfoil by rotating the end plate about its axis. A programmable microstepping motor driving the end plate via a chain drive is used for this purpose. An optical encoder on the motor shaft is used to monitor the angle of incidence to an accuracy of 0.0036 deg. The airfoil, along with its end plate and pitching mechanism, is hung from a horizontal rectangular aluminum plate supported on a pair of rails mechanically isolated from the water channel, as shown in Fig. 2. More details of the model and the support system are given in Conger and Ramaprian.[18]

Forty-one pressure taps with diameters of 1.25 mm are located along the midspan chordline of the airfoil. Fourteen of these pressure taps are located in the nose region ($x/c \leq 0.15$), one at the leading edge and seven along each side of the airfoil surface. The remaining 27 pressure taps are located along one side of the airfoil only. Pressure- and suction-side data are obtained by pitching the airfoil in opposite directions. The pressure taps communicate with the external pressure transducer via stainless and Tygon tubing.

Experimental Procedure

Pressures were measured by using a differential diaphragm-type pressure transducer connected between a reference static pressure tap and a surface pressure port via a scanning valve. Detailed studies of the dynamic response of this system, reported in Conger and Ramaprian,[19] showed that, over the experimental range of interest to this paper, the measurement system introduces negligible attenuation and less than a degree of phase shift. These small distortions were, nevertheless, corrected using the procedure developed in Ref. 19.

The main series of tests performed included 1) steady-state experiments at Reynolds numbers in the range 10^5 to 2.2×10^5, 2) pitchup experiments at $\alpha^+ = 0.072$ for different

Reynolds numbers in the range of 0.52×10^5 to 2.2×10^5, and 3) pitchup experiments at $Re = 1.3 \times 10^5$ for different values of α^+ in the range 0.036–0.2.

In addition to the aforementioned main experiments, additional experiments were conducted to study and explain some of the interesting aspects of the flow behavior observed in the main experiments. These will be described and discussed later in the paper.

The experimental procedure, in general, consisted of first setting the airfoil at a predetermined initial angle of incidence and executing a constant-rate pitching motion to a given final angle (50 deg in the pitchup tests), though data acquisition was stopped well before the cessation of motion (40 deg in the pitchup tests). Pressure vs angle data were obtained at a selected pressure tap during the pitching motion. For each experiment, results were ensemble averaged over four independent realizations (a compromise between experimental run time and accuracy). Data were obtained successively at each of the 41 pressure taps, first for clockwise pitching and next for counterclockwise pitching. These data were then smoothed and corrected, if necessary, for dynamic response. These processed data were used to obtain the distributions of the phase-locked C_p vs x/c for prescribed angles of attack. The pressure data were used to calculate the aerodynamic forces and moments.

It should be noted that the large scale and rather low aspect ratio of the model were dictated by the two major criteria: 1) to provide a fine spatial resolution of pressure measurement along the surface and 2) to obtain as large Reynolds numbers as feasible in the water channel. These conditions required some compromise to be made with respect to the blockage effect and the two-dimensionality of the flow at large angles of incidence. No standard procedure exists for the estimation of the blockage effects on pressure measurements on an airfoil,

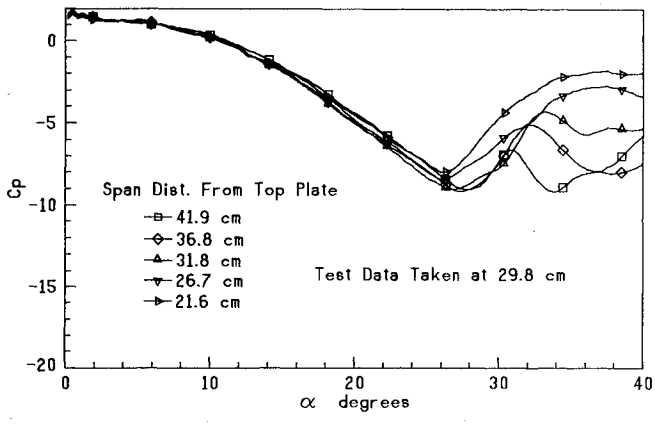

Fig. 3 Pressure vs incidence at different spanwise locations.

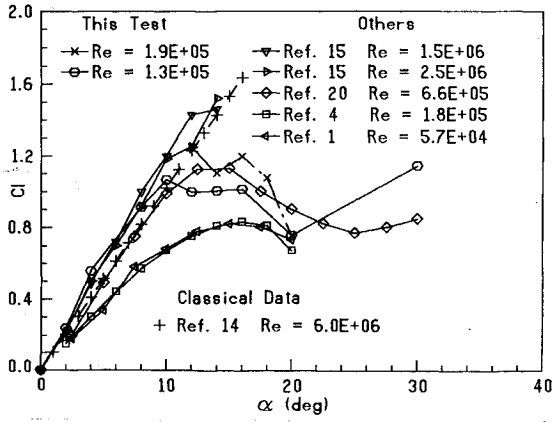

Fig. 4 Comparison of reported steady-state lift curves for the NACA 0015 airfoil.

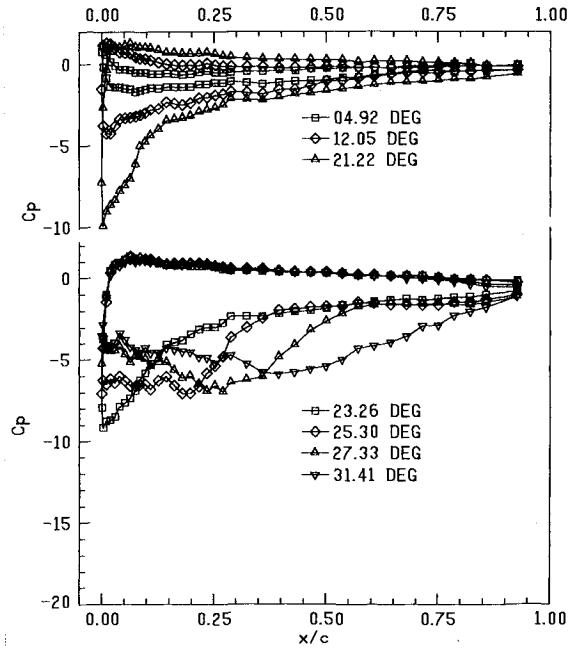

Fig. 5 Pressure distribution over the airfoil: $Re = 5.2 \times 10^4$ and $\alpha^+ = 0.072$.

especially in the case of unsteady flow. However, worst-case estimates of blockage effects were made using a method based on Ref. 15. These showed less than a 15% increase in C_l for incidences less than 20 deg and a 25% increase at 28 deg. Note that these corrections are approximate conservative estimates, and the actual typical effects are much smaller.

Similarly, from detailed measurements made in several spanwise planes, three-dimensional effects were found to be small ($< \pm 4.3\%$ variation in the maximum value of C_p over a spanwise length of $0.6c$) for incidences below 26 deg. This is typically illustrated in Fig. 3, which shows the variation of C_p with α at the nose of the airfoil at five different spanwise locations over the middle third of the span. Since the C_p vs α traces shown correspond not only to different spanwise locations but also to different pitching realizations, the figure also confirms that the flow is acceptably repetitive (at least at incidences below 26 deg). This justifies the process of ensemble averaging over just four realizations to obtain the phase-locked distributions of the surface pressure. Obviously, this procedure is not very satisfactory beyond the inception of dynamic stall.

The previous discussions with respect to blockage and three-dimensionality show that these effects are not very significant at small incidences. Hence, they do not affect the results of this study, since the focus of these experiments is on the flow up to the inception of dynamic stall, which occurs in most of the cases studied at incidences of less than 25 deg. Hence, and in view of the uncertainty of the correction methods in unsteady flow, the data presented in this paper have not been corrected for these effects except where specifically indicated otherwise.

Apart from the aforementioned, the estimated experimental uncertainties in the data (due to random errors) are as follows: C_p, $\pm 6\%$; C_l, $\pm 6\%$; and α, ± 0.07 deg.

Results

Steady-State Experiments

Figure 4 shows a comparison of the present lift data with other data available for the NACA 0015 airfoil, including the classical data from Abbot and Von Doenhoff.[13] It is evident from the comparisons in Fig. 4 that not only do the maximum lift coefficients vary for different experiments but also the slopes of the lift curves show some spread in the prestall flow

regime. The data from the present experiment lie between the classical data of Ref. 13 and the recent data of Ref. 15, both corresponding to very much higher Reynolds numbers. This is in contrast with the data of Refs. 1 and 4 (which are typical of the steady-state results from recent low-Reynolds-number unsteady-flow experiments), both of which show a considerably smaller lift slope. This difference is significant and will be discussed later in this paper.

Pitchup Tests

Reynolds Number Effects

Figures 5 and 6 show the distributions of phase-locked C_p vs x/c at different instantaneous angles of attack. The results are shown for a constant pitch rate $\alpha^+ = 0.072$ and for the lowest and highest Reynolds numbers studied. These plots exhibit an initial leading-edge suction peak located at about 1% of the chord from the nose that rapidly grows with incidence until approximately 21–24 deg (the exact angle depending on the Reynolds number). During its growth, the x/c position of the peak shifts forward, almost to the nose. It can be seen that this peak has a much larger magnitude and occurs at larger α in the higher Reynolds number experiment. After this initial growth, there is a sudden collapse of this peak. Simultaneously, a secondary suction peak forms at $x/c \approx 0.2$. Comparison with the velocity field around the airfoil (obtained in a separate study described in Ref. 16) indicates that this peak begins to form at about the same time that the boundary layer begins to detach from the airfoil surface, forming a free shear layer.

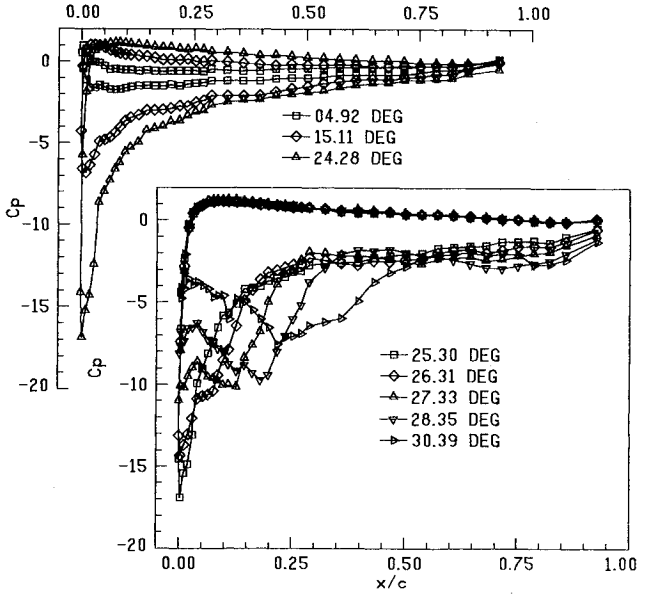

Fig. 6 Pressure distribution over the airfoil: $Re = 2.2 \times 10^5$ and $\alpha^+ = 0.072$.

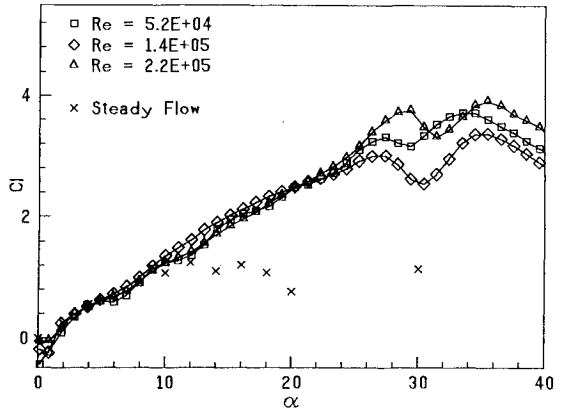

Fig. 7 Variation of the lift coefficient with Re: $\alpha^+ = 0.072$.

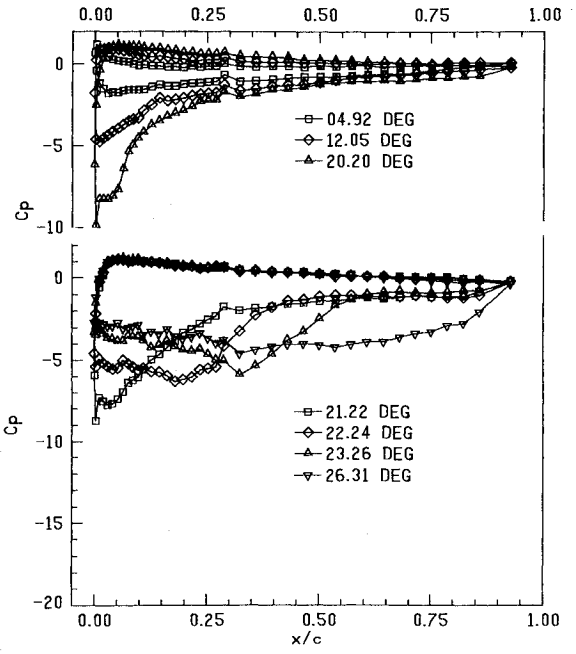

Fig. 8 Pressure distribution over the airfoil: $Re = 1.3 \times 10^5$ and $\alpha^+ = 0.036$.

The secondary peak reaches a magnitude of about three-fourths of that of the first suction peak, after which it slowly spreads out and moves downstream as the angle of attack increases further.

Although the magnitudes of these peaks seem to vary significantly with Reynolds number, the aerodynamic forces and moments obtained from integration of the surface pressure distribution showed less spectacular Reynolds number effects. This is seen from the typical plot of the lift coefficient C_l shown in Fig. 7. It is seen that Reynolds number effects are significant only beyond about 23 deg, i.e., only after the occurrence of the second suction peak associated with large-scale boundary-layer separation. It is also seen that unsteady lift curves for this pitch rate of $\alpha^+ = 0.072$ nearly coincide with the steady lift curve until $\alpha = 10$ deg. In fact, the unsteady lift curves remain nearly linear until about $\alpha = 23$ deg. The results for drag and pitching moments showed similar trends. They were found to remain small in magnitude until $\alpha \approx 23$ deg, beyond which they increased rapidly. These results are presented in Ref. 18.

The aforementioned observations from the present experiments are generally consistent with previous observations on pitching airfoils, reported in Refs. 2, 3, and 8. In particular, Ref. 3 describes a C_p distribution evolution very similar to that observed in the present experiments. However, this reference and many previous tests exhibit the presence of a "plateau" located near the nose that may stretch over a length of the suction surface up to 10–15% of the chord. This behavior is not seen in the present data shown in Figs. 5 and 6.

Pitch Rate Effects

The effect of pitch rate on the pressure distribution is presented in Figs. 8 and 9, which show the results for two typical pitch rates, $\alpha^+ = 0.036$ and 0.2. These curves are qualitatively similar to those previously discussed for $\alpha^+ = 0.072$. However, it can be seen that increased pitch rate has the effect of 1) increasing the overall C_p values, 2) defining the suction peaks more clearly, and 3) delaying collapse of the initial pressure peak to larger incidences. In the first two respects, increasing the pitch rate has much the same effect as increasing the Reynolds number. In case 3, although a similar delaying trend was observed for increased Reynolds number, the effect of pitch rate is seen to be far more pronounced. Notice that the maximum suction peak changes from about -10 at

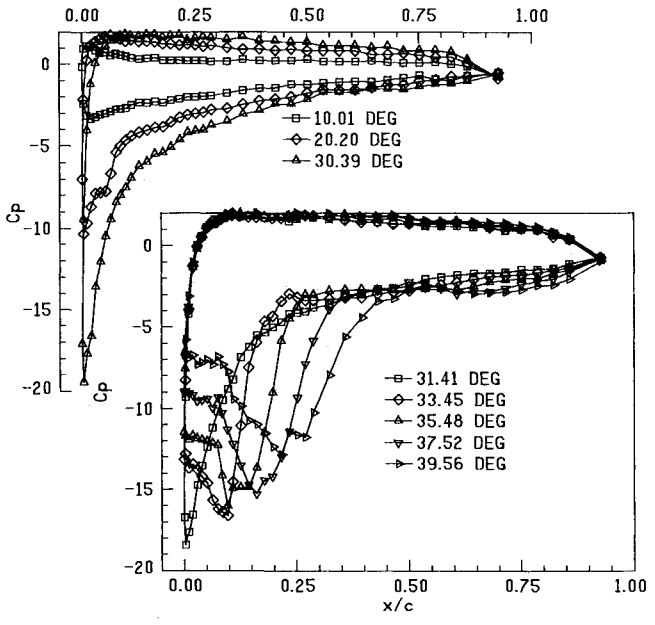

Fig. 9 Pressure distribution over the airfoil: $Re = 1.2 \times 10^5$ and $\alpha^+ = 0.200$.

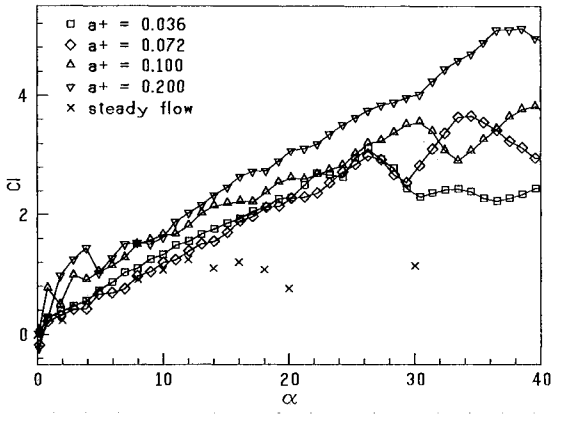

Fig. 10 Variation of the lift coefficient with α^+: $Re \approx 1.3 \times 10^5$.

the lower pitch rate to about -20 at the higher pitch rate (even though blockage effect might have slightly exaggerated the difference). At the lowest pitch rate of $\alpha^+ = 0.036$ studied, a small pressure plateau is seen near the nose of the airfoil. This is, however, much smaller in size than those reported in earlier studies. This plateau was found to vanish gradually as the pitch rate was increased. In fact, at the highest pitch rate of $\alpha^+ = 0.2$ studied, it can be detected only as a slight inflection in the C_p distribution in the nose region.

Figure 10 gives the C_l vs α curves for different pitch rates. Most obviously, the apparent maximum C_l occurs at a higher incidence and has a larger magnitude at higher pitch rates. From an examination of Figs. 8–10, it can be seen that at all pitch rates the value of C_l reaches a peak slightly after the secondary suction peak appears. The second higher C_l peak seen in the case of the two intermediate pitch rates is perhaps spurious and is possibly due to blockage effects. In fact, the data shown for incidences larger than 30 deg should be interpreted with caution in all cases.

It is also seen that at higher pitch rates the lift curve is shifted above that of the steady-state lift curve. In fact, a positive lift can be seen at $\alpha = 0$ by extrapolating the linear portion of the lift curve backwards to zero incidence (and thereby ignoring the wiggles in data points near $\alpha = 0$, which may represent transient effects arising from the impulsive start of motion). This shift represents the departure of the flow from quasisteady behavior, which should be expected to become significant as the Strouhal number α^+ becomes larger. This and other features of the unsteady flow are discussed in more detail in the next section.

Additional Studies and Discussion

Role of Freestream Turbulence and Imposed Unsteadiness

In general, the present results compare very well qualitatively with previous experimental and numerical studies of pitching airfoils at similar or lower Reynolds numbers with regard to the behavior of the surface pressure and aerodynamic forces. However, the present data do show significant departure from earlier studies with respect to the magnitudes of the measured pressures and forces. The present suction peak and maximum C_l values are, in general, significantly larger than the earlier values reported for similar Reynolds numbers and pitch rates. Although some of this difference can be attributed to blockage effects in the present experiment, blockage is not the major cause. In fact, at least one experiment with larger blockages (Ref. 2) has reported much lower C_p values. Also, note that corrections for blockage become significant in most tests only beyond the angle corresponding to the suction peak and hence cannot explain the large suction peak in the present experiment. In any case, the corrections are not large enough to reduce the present lift values to those reported in previous studies. This is clearly seen from Fig. 11, which shows a comparison of the present data (before and after correction for blockage effects) with those of Refs. 9 and 11. Similar arguments hold for three-dimensional effects also. In fact, in general, three-dimensional effects tend to reduce the measured value of the suction peak rather than increase it and thus cancel to some extent the blockage effects. It thus seems reasonable to conclude that the large magnitudes of the suction peaks and lift coefficients measured in the present experiments are primarily caused by a more fundamental mechanism in the flow. This conclusion is strengthened by reference to the experiments of Ref. 5 (albeit on a Sikorsky SSC-A09 airfoil) at high Reynolds numbers ($2\text{–}4 \times 10^6$) that yielded suction peaks comparable to the present measurements at similar and lower pitch rates.

The feature that distinguishes the present experiments from the earlier wind-tunnel and towing-tank experiments is the rather high freestream turbulence (0.8–1%) in the water channel. It is known that such high levels of turbulence can induce very early laminar-turbulent transition in the boundary layer. Furthermore, it is known from earlier studies on unsteady turbulent boundary layers[21] that any imposed unsteadiness can trigger transition in flows at near-transitional Reynolds numbers. In fact, this triggering is almost instantaneous, and the effect is not strongly dependent on the time scale of unsteadiness imposed, *as long as the flow is near transitional*. If such a transition is occurring in the present experiments, it would cause the resulting turbulent boundary layer to remain attached and thus suppress the formation of a separation "bub-

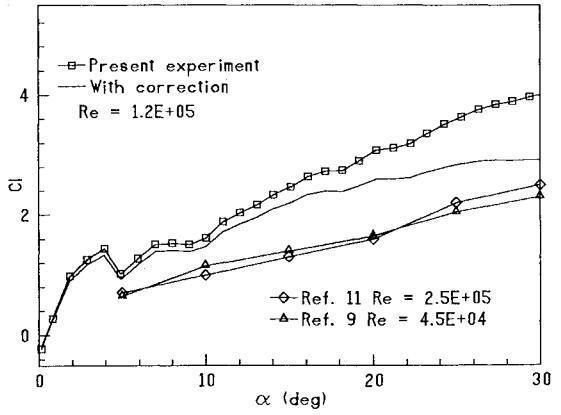

Fig. 11 Comparison of reported unsteady lift data with the present data and blockage correction: $\alpha^+ = 0.200$.

ble" on the suction side of the airfoil. Even if this transition was incomplete, it would at least act to reduce greatly the size of this separation bubble.

In fact, the role of transition and separation bubble in significantly reducing the lift in steady flows at Reynolds numbers on the order of 10^5 is well known. Lissaman[22] estimates that in a flow at $Re = 5 \times 10^4$ the length of the separation bubble is on the order of the airfoil chord, thus completely preventing turbulent reattachment and drastically reducing the airfoil performance. The reduced values of steady-state pressures and lift forces measured in the earlier low-Reynolds-number studies can be ascribed to the aforementioned reason.

It is hypothesized here that the high freestream turbulence in the water channel, combined with the imposed unsteadiness during pitching, promoted very early transition in the present experiments, thus either completely eliminating the separation region or drastically reducing its size. This has resulted in a flow behavior comparable to that at much higher Reynolds numbers ($Re \approx 10^6$). On the other hand, it is very likely that in the earlier low-Reynolds-number experiments, in the absence of high freestream turbulence, the flow was not near transition. Hence, even the imposed unsteadiness in those experiments was apparently unable to trigger rapid transition in the flow near the leading edge, which would result in the occurrence of a sizable separation bubble. The presence of a pressure plateau in many of the earlier pitching airfoil tests may, in fact, be the signature of this bubble. The small plateau observed in Fig. 8a at the low pitch rate of $\alpha = 0.036$ is closer to the nose and shorter than those observed in other experiments and thus may be the signature of a small separation bubble that was not quite eliminated by the relatively weak unsteady effects in this experiment.

Pitchup and Hold Tests

To assess the validity of the previous hypothesis, some special additional experiments were performed. In these experiments, the airfoil was subjected to a "pitchup and hold" maneuver. Figure 12 shows the results of such tests. In these tests, which were performed at a freestream velocity of 30 cm/s, the airfoil was held at zero incidence for about 30 s from the beginning of the test, then pitched at constant angular velocity (corresponding to $\alpha^+ \approx 0.1$) for about 2 s to a final angle of incidence, and held there for a very long time. The experiment was repeated several times. The variation of the pressure at the nose tap with time is shown for each realization. Also shown are typical instantaneous streamline patterns around the suction side of the airfoil, obtained from PIV. The light line in Fig. 12 corresponds to the case when the final angle of incidence was 18 deg (poststatic stall), and the dark lines correspond to the case when the final angle was 16 deg (near-static stall).

From the data for the 18-deg incidence, it is seen that C_p at the nose starts at the steady-state stagnation value of 1.0 and attains the maximum negative value of about -5.2 at the end of the pitchup motion. This is the expected value at this x/c location at an incidence of 18 deg at this Reynolds number and pitch rate. The flow remains attached to the forebody surface throughout this motion. As soon as the pitching is stopped, the value of C_p drops to about -0.8, which is the value appropriate to the poststall angle of 18 deg in steady flow at this x/c location. This drop occurs in a time period of about 20 s corresponding to $U_\infty t/c \approx 19$ (i.e., about 19 convection times). That the final flow is separated is clearly seen from the corresponding streamline pattern shown in the figure. This was obtained from an actual measurement of the instantaneous velocity field using PIV. Virtually identical behavior of the C_p distribution was observed in *all* of the realizations when this test was repeated.

The pitch-and-hold experiments at 16 deg show a significantly different behavior. In all realizations, when the pitching is stopped at 16 deg (which corresponds to the static-stall angle), the value of C_p changes from about -4.4 (corresponding to the unsteady flow at 16-deg incidence) to a value of about 3.6 over a period corresponding to about 19 convective times. After this, the behavior of the flow is unpredictable. In some realizations, it stays in this condition for a very long time ($U_\infty t/c \geq 150$). In some cases, after a considerably shorter period of time, it reverts to the stalled steady-state value on its own. Simultaneous PIV measurements showed that in the first case the flow in the forebody region was attached, whereas in the second case it was separated. This is seen from the corresponding streamline patterns shown. It was found that even a vigorous external agitation of the upstream flow would not cause the attached flow to separate in the first case. It was also found that the duration of the attached state could be an order of magnitude larger than the characteristic convection time for the model in the channel. It seems reason-

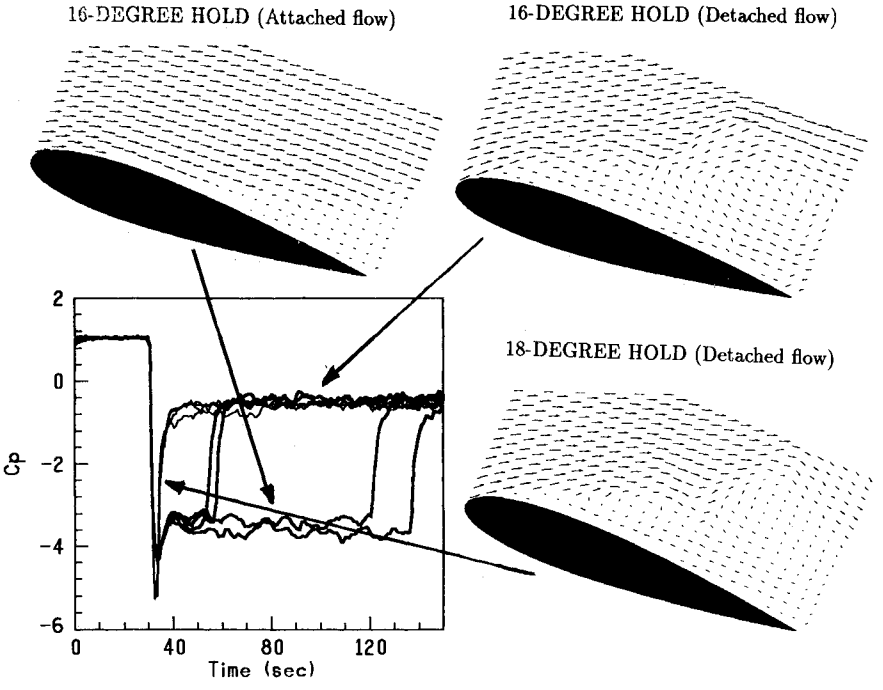

Fig. 12 Results from the pitch-and-hold experiments.

able to conclude that the two possible states can be identified as attached turbulent and separated (stalled) laminar flow, respectively.

It was also found that the previous results were not dependent on the exact value of the pitching rate or acceleration/retardation at the start/end of the pitching motion. If the final angle of incidence in the previous tests was less than 16 deg, the flow remained attached all of the time, with the value of C_p just changing from the unsteady to the quasisteady value at the end of pitching.

It is thus clear now that the reason for the simulation of high-Reynolds-number flow in the present facility is the triggering of transition by the unsteadiness even at low pitching rates in the flow that is rendered transitional because of the high freestream turbulence. One can thus regard the combination of these conditions as being equivalent to a "giant tripping device" that promotes rapid transition. It should, however, be noted that the simulation of high Reynolds number flow is limited to the regime of attached boundary-layer flow. Beyond this regime, Reynolds number effects may become significant because of the greater role played by the viscous/turbulent effects in the vortical region. It is therefore possible that the subsequent evolution of the dynamic stall vortex and the maximum lift attained may not be correctly simulated in these experiments.

Quasisteady and Dynamic Effects of Pitching

The bimodal nature of the final state confirms that it is controlled by transition. The correspondence of the C_p values at the end of pitching with the steady-state value for the attached (turbulent) flow, except for the small difference between the quasisteady and unsteady values, confirms that the unsteadiness imposed during pitching triggers transition almost instantaneously and causes the resulting turbulent boundary layer to remain attached beyond the normal steady-stall incidence. If pitching is continued beyond 16 deg in the present facility, the boundary layer would continue to remain attached and the suction peak and lift force would continue to increase because of the generation of net clockwise vorticity by the unsteady pressure gradient at the surface. This increase would continue until viscous effects become very strong at an elevated incidence and interfere with this process. At smaller pitch rates the process would be nearly quasisteady and the resulting lift curve would be very nearly the extension of the steady-state lift curve, until viscous effects become very strong. The pitch rate simply determines the point beyond which the viscous effects become important. At higher pitch rates, however, dynamic effects become significant, resulting in the displacement of the lift curve, as already discussed with reference to Fig. 10. The non-quasisteady effects, however, are not spectacular even at $\alpha^+ = 0.2$. In fact, the maximum suction peak values show almost quasisteady behavior even up to this pitch rate, as long as the turbulent boundary layer remains attached. This is vividly seen from Fig. 13, which shows the variation of suction peak as a function of α at different pitch rates. It is seen that when the boundary layer remains attached (i.e., approximately up to the incidence corresponding to the maximum suction peak), the magnitude of the suction peak is independent of the pitch rate. It was also found that as long as the turbulent boundary layer remains attached, the pressures and forces are not drastically affected by Reynolds number either. Details of these results are presented in Ref. 18.

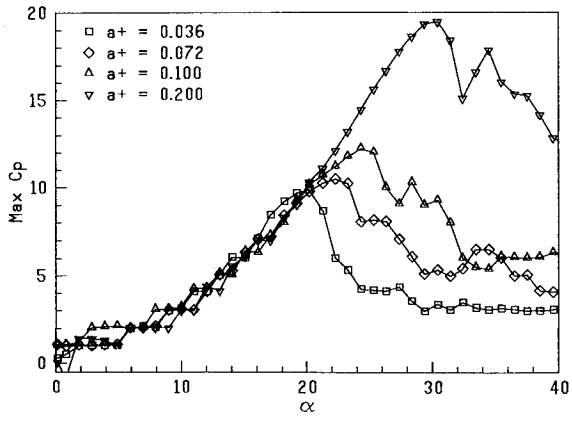

Fig. 13 Maximum negative C_p vs α at four different pitch rates.

Conclusions

An investigation into the development of the pressure distributions over the pitching airfoil has identified a behavior that is qualitatively consistent with previous observations. However, the magnitudes of the pressures and aerodynamic forces measured in this study were found to be significantly larger than those reported from earlier studies performed at similar low Reynolds numbers. A careful study shows that this is most likely due to the early and rapid triggering of laminar-turbulent transition in the flow, thereby suppressing the so-called separation bubble or greatly limiting its size and causing the resulting turbulent boundary layer to remain attached to the surface. This is caused by the combination of high freestream turbulence (relative to the other experiments) and imposed unsteadiness during pitching. This effective "tripping" resulted in the simulation of much higher Reynolds number effects in the present flow. The experiments also showed that as long as the boundary layer remains attached, the most dominating effect of pitching, especially at small pitch rates, is the extension of the steady lift curve beyond the static-stall angle, in a quasisteady manner. Pitch rate and Reynolds number only determine the maximum angle of incidence up to which the boundary layer remains attached. The dynamic effects become significant only at higher pitch rates ($\alpha^+ > 0.1$). In the absence of the separation bubble, pitch rate and Reynolds number effects become important mainly beyond the point of maximum suction peak (i.e., after the boundary layer detaches to form a free shear layer) when the dynamic stall vortex appears and evolves.

The apparent simulation of high-Reynolds-number flow conditions in the water channel is an attractive feature that allows detailed pressure data to be obtained to a degree of spatial and temporal resolution that would be very difficult and expensive, even if not impossible, to achieve in a large wind tunnel. All of the present data are archived and will be made available to any interested reader.

Acknowledgments

This project was supported by the U.S. Air Force Office of Scientific Research, under Grants AFOSR 90-0131 and F49620-92-J-0146, with (initially) H. Helin and (subsequently) D. Fant as program managers.

References

[1]Albertson, J. A., Troutt, T. R., Siriu, W. D., and Walker, J. M., "Dynamic Stall Vortex Development and the Surface Pressure Field of a Pitching Airfoil," AIAA Paper 83-133, Jan. 1983.

[2]Acharya, M., and Metwally, M. H., "Evolution of the Unsteady Pressure Field and Vorticity Production at the Surface of a Pitching Airfoil," AIAA Paper 90-1472, June 1990.

[3]Francis, M. S., and Keesee, J. E., "Airfoil Dynamic Stall Performance with Large-Amplitude Motions," *AIAA Journal,* Vol. 23, No. 11, 1985, pp. 1653–1659.

[4]Jumper, E. J., Schreck, S. J., and Dimmick, R. L., "Lift-Curve Characteristics for an Airfoil Pitching at Constant Rate," *Journal of Aircraft,* Vol. 24, No. 10, 1987, pp. 680–687.

[5]Lorber, P. F., and Carta, F. O., "Unsteady Stall Penetration Experiments at High Reynolds Number," United Technologies Research Center, UTRC Rept. R87-956939 (AFOSR TR-87-1202), East Hartford, CT, April 1987.

[6]Shih, C., Lorenco, L., Van Dommeien, L., and Krothapalli, A., "Unsteady Flow Past an Airfoil Pitched at Constant Rate," *International Symposium on Nonsteady Fluid Dynamics,* edited by J. A.

Miller and D. P. Telionis, Vol. 92, Fluids Engineering Division, American Soc. of Mechanical Engineers, New York, 1990, pp. 41–50.

[7]Visbal, M. R., "On the Formation and Control of the Dynamic Stall Vortex on a Pitching Airfoil," AIAA Paper 91-0006, Jan. 1991.

[8]Visbal, M. R., and Shang, J. S., "Investigation of the Flow Structure Around a Rapidly Pitching Airfoil," *AIAA Journal,* Vol. 27, No. 8, 1989, pp. 1044–1051.

[9]Walker, J. M., Helin, H. E., and Chou, D., "Unsteady Surface Pressure Measurements on a Pitching Airfoil," AIAA Paper 85-0532, March 1985.

[10]Walker, J. M., Helin, H. E., and Strickland, J. H., "An Experimental Investigation of an Airfoil Undergoing Large Amplitude Pitching Motions," *AIAA Journal,* Vol. 23, No. 8, 1985, pp. 1141–1143.

[11]Graham, G. M., and Yeow, K. F., "Two-Dimensional Post Stall Maneuver of a NACA 0015 Airfoil at High Pitching Rates," AIAA Paper 90-2810, June 1990.

[12]Strickland, J. H., and Graham, G. M., "Force Coefficients for a NACA-0015 Airfoil Undergoing Constant Pitch Rate Motions," *AIAA Journal,* Vol. 25, No. 4, 1987, pp. 622–624.

[13]Abbot, I. H., and Von Doenhoff, A. E., *Theory of Wing Sections: Including a Summary of Airfoil Data,* Dover, New York, 1949, pp. 129–324.

[14]Piziali, R. A., personal communication, NASA Ames Research Center, Moffett Field, CA, 1992.

[15]McAlister, K. W., and Takahashi, R. K., "NACA 0015 Wing Pressure and Trailing Vortex Measurements," NASA TP 3151, 1991; also AVSCOM TR 91-A-003, Nov. 1991.

[16]Oshima, H. O., and Ramaprian, B. R., "Measurement of the Velocity and Vorticity Fields Around a Pitching Airfoil," AIAA Paper 92-2626, June 1992.

[17]Conger, R. N., and Ramaprian, B. R., "The WSU-MME 1 m $\times$ 0.7 m Water Channel," Dept. of Mechanical and Materials Engineering, Washington State Univ., Rept. MME-TF-92-1, Pullman, WA, May 1992.

[18]Conger, R. N., and Ramaprian, B. R., "Pressure Measurements on a Pitching Airfoil in a Water Channel," Dept. of Mechanical and Materials Engineering, Washington State Univ., Rept. MME-TF-92-3, Pullman, WA, May 1992.

[19]Conger, R. N., and Ramaprian, B. R., "Correcting for Response Lag in Unsteady Pressure Measurements," *Journal of Fluids Engineering* (to be published).

[20]Shehdahl, R. E., and Klimas, P. C., "Aerodynamic Characteristics of Seven Symmetric Airfoil Sections Through 180 Degree Angle of Attack for Use in Aerodynamic Analysis of Vertical Axis Wind Turbines," Sandia National Lab., Rept. SAND80-2114, 1981.

[21]Menendez, A. N., and Ramaprian, B. R., "Experimental Study of a Periodic Turbulent Boundary Layer in Zero Mean Pressure Gradient," *Aeronautical Journal,* Vol. 93, No. 926, 1989, pp. 195–206.

[22]Lissaman, P. B. S., "Low-Reynolds Number Airfoils," *Annual Reviews of Fluid Mechanics,* Vol. 15, 1983, pp. 223–229.